JOURNAL OF VIROLOGY, Dec. 2005, p. 15302–15313 Vol. 79, No. 24
0022-538X/05/$08.00+0 doi:10.1128/JVI.79.24.15302–15313.2005

Respiratory Syncytial Virus-Inducible BCL-3 Expression Antagonizes the STAT/IRF and NF-κB Signaling Pathways by Inducing Histone Deacetylase 1 Recruitment to the Interleukin-8 Promoter

Mohammad Jamaluddin,[1] Sanjeev Choudhary,[1,6] Shaofei Wang,[1] Antonella Casola,[2] Ruksana Huda,[5] Roberto P. Garofalo,[2,3] Sutapa Ray,[1] and Allan R. Brasier[1,4]*

Departments of Medicine,[1] Pediatrics,[2] Microbiology and Immunology,[3] Anesthesiology,[5] and Human Biological Chemistry and Genetics[6] and Sealy Center for Molecular Sciences,[4] The University of Texas Medical Branch, Galveston, Texas 77555-1060

Received 8 July 2005/Accepted 8 September 2005

Respiratory syncytial virus (RSV) is a paramyxovirus that produces airway inflammation, in part by inducing interleukin-8 (IL-8) expression, a CXC-type chemokine, via the NF-κB/RelA and STAT/IRF signaling pathways. In RSV-infected A549 cells, IL-8 transcription attenuates after 24 h in spite of ongoing viral replication and persistence of nuclear RelA, suggesting a mechanism for transcriptional attenuation. RSV infection induces B-cell lymphoma protein -3 (Bcl-3) expression 6 to 12 h after viral infection, at times when IL-8 transcription is inhibited. By contrast, 293 cells, deficient in inducible Bcl-3 expression, show no attenuation of IL-8 transcription. We therefore examined Bcl-3's role in terminating virus-inducible IL-8 transcription. Transient expression of Bcl-3 potently inhibited virus-inducible IL-8 transcription by disrupting both the NF-κB and STAT/IRF pathways. Although previously Bcl-3 was thought to capture 50-kDa NF-κB1 isoforms in the cytoplasm, immunoprecipitation (IP) and electrophoretic mobility shift assays indicate that nuclear Bcl-3 associates with NF-κB1 without affecting DNA binding. Additionally, Bcl-3 potently inhibited the STAT/IRF pathway. Nondenaturing co-IP assays indicate that nuclear Bcl-3 associates with STAT-1 and histone deacetylase 1 (HDAC-1), increasing HDAC-1 recruitment to the IL-8 promoter. Treatment with the HDAC inhibitor trichostatin A blocks attenuation of IL-8 transcription. A nuclear targeting-deficient Bcl-3 is unable to enhance HDAC-1-mediated chemokine repression. Finally, small inhibitory RNA-mediated Bcl-3 "knockdown" resulted in enhanced RSV-induced chemokine expression in A549 cells. These data indicate that Bcl-3 is a virus-inducible inhibitor of chemokine transcription by interfering with the NF-κB and STAT/IRF signaling pathways by complexing with them and recruiting HDAC-1 to attenuate target promoter activity.

Respiratory syncytial virus (RSV), a negative-sense RNA virus of the *Paramyxoviridae* family, is the leading cause of epidemic bronchiolitis and pneumonia in children (38). Lacking an effective vaccine, infection with this ubiquitous virus causes 40 to 60% of the bronchiolitis and 15 to 25% of the pneumonia cases in hospitalized children (40, 53), accounting for ~100,000 hospitalizations and ~500 deaths annually in the United States (41). Infection is initiated by contact with viral particles contained within contaminated secretions and the nasopharyngeal epithelium (19). Replicating virus subsequently spreads to the lower respiratory tract via apical cell-to-cell transfer along ciliated epithelial cells of the conducting airways (59). In infants and immunocompromised patients who develop severe lower respiratory tract infection, RSV induces infiltration of mononuclear cells and lymphocytes into the peribronchial and perivascular spaces (1, 15, 16).

Cellular recruitment into the virally infected lung is a multistep process involving adherence of circulating leukocytes to an activated endothelial surface, followed by their diapedesis and migration toward chemical gradients of chemoattractant peptides or antigens (reviewed in reference 45). Recent attention has focused on the important role of chemokines in mediating leukocyte chemotaxis into the airways. Chemokines are a superfamily of proteins divided into four distinct groups, C, CC, CXC, and CX_3C (based on the number and spacing of highly conserved NH_2-terminal cystine residues [reviewed in references 3 and 33]) that bind cell surface leukocyte receptors, producing activation and chemotaxis of distinct cellular subsets. Our recent studies using high-density oligonucleotide arrays have shown that RSV-infected airway epithelium can express at least 16 different C, CC, CXC, and CX_3C chemokines (62), making it an important cell type in initiating airway inflammation. The molecular mechanisms controlling expression of CXC- and CC-type chemokines in RSV-infected airway epithelial cells have been extensively investigated (5, 10, 12, 17, 50, 51). Interleukin-8 (IL-8), found in increased levels in the plasma of RSV-infected children that correlate with disease severity, is a prototypical CXC chemokine that is a potent neutrophil chemoattractant (30).

In epithelial cells, RSV replication induces IL-8 expression through enhanced transcription initiation, a process mediated primarily by inducible nuclear factor κB (NF-κB) and signal transducers and activators of transcription (STAT)/interferon response factor (IRF) transcription factors that interact in a multiprotein complex termed the "enhanceosome" (9, 49). NF-κB is a cytoplasmic transcription factor whose activity is induced by RSV through two mechanistically and temporally distinct activation pathways; early in the process of RSV infection, NF-κB is activated by a "noncanonical" pathway medi-

* Corresponding author. Mailing address: Division of Endocrinology, MRB 8.138, The University of Texas Medical Branch, 301 University Blvd., Galveston, TX 77555-1060. Phone: (409) 772-2824. Fax: (409) 772-8709. E-mail: arbrasie@utmb.edu.

ated by the NF-κB-inducing kinase, a kinase responsible for an early, but weak transcriptional response, and later the canonical pathway is activated, mediated by releasing the more potent NF-κB/RelA transactivator from its sequestered cytoplasmic location (12). The canonical pathway is the result of calpain- and proteosome-mediated proteolysis of inhibitory ankyrin repeat-containing proteins, including the IκBα and -β subunits. IκB proteolysis allows NF-κB/RelA to enter the nucleus and bind to high-affinity genomic sites, activating expression of a genetic network whose activities are important in immuno-modulation and inflammation (17, 23, 51). NF-κB binding is absolutely required for IL-8 transcription, because mutations that block NF-κB binding render the promoter inert to stimulation (17), and inhibition of NF-κB translocation blocks RSV-induced IL-8 expression (51).

In addition to NF-κB, the STAT/IRF pathway controls a distinct, but interrelated, arm of the innate response to viral replication. STATs are cytosolic proteins activated by tyrosine phosphorylation mediated either by the interferon/growth factor receptor-associated kinases, Jak and Tyk (reviewed in reference 39), or by virus-induced alterations in phosphatase activity (11). Activated STATs then form homo- or heterodimers through intermolecular SH2 phosphotyrosine interactions and are subsequently translocated into the nucleus in distinct binding complexes dictated by the nature of the stimulus and target promoters (13). In conjunction with NF-κB, STATs control important cellular genes involved in the epithelial response to RSV, including the inducible interferon response factor 1 (IRF-1) and IRF-7 isoforms. In particular, on the IRF-1 gene, STAT-1 and -3 form a complex that binds to the viral inducible GAS sequence, a site required for IRF-1 expression that interacts with an adjacent NF-κB site (26), further illustrating the interrelated nature of these two pathways. IRF-1 expression in turn is required for IL-8 expression, forming a multiprotein binding complex on the RSV-inducible response element (RSVRE) (9). Mutagenesis studies have shown that the IRF binding to the RSVRE is required for IL-8 promoter induction after RSV infection, even in the presence of an intact NF-κB binding site (9). These studies indicate that virus-inducible IL-8 transcription is mediated through the NF-κB and STAT/IRF pathways, pathways that play a central role in the control of virus-induced chemokine expression (51) and lung inflammation (4, 18).

Recently, a body of work has indicated that counter-regulatory proteins are important in terminating the action of inducible transcription factor pathways (46, 57). For example, the NF-κB-dependent resynthesis of IκBα is a mechanism for recapturing nuclear NF-κB into the cytoplasm and terminating its action, known as the NF-κB–IκBα feedback loop (47). However, our previous work indicated the NF-κB–IκBα feedback loop is significantly attenuated in RSV infection because IκBα is not detectably resynthesized, in contrast to the effect of tumor necrosis factor (TNF) in the same cells (23). However, we suspected other ankyrin repeat-containing proteins were induced by RSV infection, because NF-κB transcriptional activity is transient in spite of ongoing RSV infection (17). By observing differences in transcriptional profiles of two cell types that differentially express the B-cell lymphoma 3 (Bcl-3) protein, we report here our studies describing its role in terminating chemokine transcription. In A549 cells, RSV infection induces Bcl-3 expression, at times preceding inhibition of NF-κB-dependent promoter activity. In probing its site of action, we found that Bcl-3 is an inhibitor of NF-κB-dependent transcription but, interestingly, is a more potent inhibitor of STAT transcriptional activity. We therefore further investigated this mechanism and found that Bcl-3 bridges an association with STAT-1 and histone deacetylase 1 (HDAC-1), recruiting HDAC-1 to endogenous IL-8 promoters in chromatin immunoprecipitation (ChIP) assays. This phenomenon is dependent on Bcl-3 nuclear localization being deficient in a cytoplasmic targeted Bcl-3 mutation. Conversely, small inhibitory RNA (siRNA)-mediated Bcl-3 knockdown enhances chemokine expression in A549 cells. Together, these data suggest that inducible Bcl-3 synthesis is a counter-regulatory mechanism for inhibiting both the RSV-induced NF-κB and STAT/IRF pathways, pathways essential for virus-induced chemokine expression.

MATERIALS AND METHODS

Cell culture and treatment. Human alveolar type II epithelial, A549, and human embryonic kidney epithelial 293 cells (American Type Culture Collection, Manassas, Va.) were cultured in F12K and minimum essential medium, respectively, supplemented with 10% (vol/vol) fetal bovine serum, 2 mM glutamine, penicillin (100 IU/ml), and streptomycin (100 μg/ml). At 80 to 90% confluence, cells were infected with sucrose gradient-purified RSV, A2 (pRSV), at a multiplicity of infection (MOI) of 1 for different times (17). An equivalent amount of a 20% sucrose solution was added to uninfected cells as a control. Cell monolayers were treated with 20 ng of recombinant human TNF alpha (rhTNF-α; R&D Systems), 8 ng IL-6 (rhIL-6; Calbiochem), 100 IU of gamma interferon (rhIFN-γ; Boehringer Mannheim) per ml, or 0.5 μM phorbol myristate acetate (PMA; Sigma Aldrich) and incubated at 37°C. The histone deacetylase inhibitor trichostatin A (TSA; Sigma Aldrich) was used at a final concentration of 100 nM.

Plasmid construction. The RANTES ISRE multimers were made by phosphorylating the duplex sequences, 5′-GATCCATATTTCAGTTTTCTTTTCCG T-3′, and ligating them upstream of an inert IL-8 promoter (−54/+44 IL-8 LUC). Luciferase reporter genes driven by the fully inducible human IL-8 promoter (hIL-8/LUC) (6, 55) and the human IRF-1 promoter (hIRF-1/LUC) (44) were previously described. Luciferase reporters under selective control of the multimeric NF-κB, AP-1, and STAT-3 *cis* elements have also been described (6, 9, 42, 55).

Eukaryotic expression vectors. The expression plasmid encoding FLAG epitope-tagged Bcl-3, pcDNA3-FLAG-Bcl-3, was previously reported (7). A truncation mutant of Bcl-3 cDNA was generated by deletion of the N terminal (ΔN) by PCR using the wild-type plasmid as template (the BamH1 and HindIII restriction sites are italicized). The sequences of the sense and antisense primers are as follows: Bcl-3 ΔNS, 5′-GCTA*GGATCC*ATGGCCACCCGTGCAGATG AGGAC-3′; Bcl-3 ΔNA, 5′-GCTA*AAGCTT*CAGCTGCC TCCTGGAGCTGG GGAGGG-3′. The PCR products were digested with BamH1 and HindIII, purified, and ligated into pcDNA3 FLAG (7). All plasmids were sequenced to verify their authenticity.

Cell transfection. Logarithmically growing cells were transiently transfected in triplicate in 60-mm petri dishes using FuGene 6 (Roche, Indianapolis, Ind.) as previously described (9). Two micrograms of hIL-8/LUC and IRF-1/LUC plasmids, different amounts of pcDNA3-Flag-Bcl-3 expression plasmids, and 1 μg of cytomegalovirus β-galactosidase internal control plasmids were premixed with FuGene 6 in a ratio of 1:3 (μg/μl) and added to the cells in 2 ml of culture medium. The next day cells were infected with RSV at a MOI of 1. At the indicated times, cells were lysed to measure luciferase and β-galactosidase reporter activities. Luciferase activity was normalized to internal control β-galactosidase activity. All experiments were repeated at least twice in triplicate.

Western immunoblotting. Cytoplasmic and nuclear extracts were prepared as previously described. In all preparations, nuclei were washed and passed through a sucrose cushion to remove cytoplasmic contamination (8, 23). Equal amounts of cytoplasmic and nuclear protein were separated by sodium dodecyl sulfate-polyacrylamide gel electrophoresis (SDS-PAGE) and transferred to polyvinylidene difluoride membrane. The membranes were blocked in 5% nonfat dry milk in Tris-buffered saline–Tween and incubated with affinity-purified rabbit poly-

clonal antibodies to Bcl-3 (sc-185) and STAT-1 (sc-592) (Santa Cruz Biotechnology), HDAC-1 (05-614; Upstate Biotechnology), and mouse monoclonal antibodies to FLAG epitope or β-actin (Sigma Aldrich) as indicated. After washing, membranes were incubated with horseradish peroxidase-conjugated donkey anti-rabbit or anti-mouse immunoglobulin G (IgG), and immune complexes were detected by enhanced chemiluminescence (Amersham Biosciences). For the nondenaturing coimmunoprecipitation (co-IP) assays, nuclear protein from 293 cells transiently transfected with pcDNA3-FLAG-Bcl-3 plasmids was incubated with 5 μg of STAT-1 antibody (Ab; Santa Cruz Biotechnology) and 50 μl of protein A-Sepharose 4B in 1 ml of TST buffer (50 mM Tris-HCl, pH 7.5, 5 mM EDTA, 150 mM NaCl, and 0.05% Triton X-100) overnight at 4°C. The immune complex was precipitated, washed with TST, boiled in Laemmli buffer, and analyzed by Western immunoblotting as described above.

RNA analysis. For Northern blot assays, 20 μg of acid guanidium-phenol-extracted RNA was fractionated by electrophoresis on a 1.2% agarose-formaldehyde gel, transferred to nitrocellulose (Zeta-Probe GT; Bio-Rad), and prehybridized (54). The ^{32}P-labeled Bcl-3 probe was produced by 30 cycles of asymmetric PCR of the 527-bp fragment of Bcl-3 cDNA using the antisense primer 5′-GCTCAAGCTTGAGCTGCACGGTTTCTTGG-3′ in the presence of [α-^{32}P]dATP. The blot was hybridized with 10^6 cpm of ^{32}P-labeled Bcl-3 cDNA probes per ml at 62°C overnight in 5% SDS hybridization buffer and washed with 5% SDS and 1× SSC (0.15 M NaCl plus 0.015 M sodium citrate) for 20 min at room temperature followed by 30 min at 62°C. Internal control hybridization was for glyceraldehyde-3-phosphate dehydrogenase. The blot was exposed to X-AR film (Eastman Kodak Co) for 24 h at −70°C and quantified by exposure to a PhosphorImager cassette (Molecular Dynamics). For quantitative real-time PCR (Q-RT-PCR), Applied Biosystems assays-on-demand 20× mix of primers and TaqMan MGB probes (6-carboxyfluorescein dye labeled) for target genes and 18S rRNA (VIC dye-labeled probe) TaqMan assay reagent (P/N 4319413E) for controls were used. Separate tubes (single plex) were used, and a one-step RT-PCR was performed with 80 ng RNA for both target genes and endogenous control. The cycling parameters for the one-step RT-PCR were reverse transcription 48°C for 30 min, Ampli*Taq* activation at 95°C for 10 min, denaturation at 95°C for 15 s, and annealing/extension at 60°C for 1 min (repeat, 40 times) on an ABI 7000. Duplicate *Ct* values were analyzed in Microsoft Excel using the comparative *Ct* (Δ*Ct*) method as described by the manufacturer (Applied Biosystems). The amount of target ($2^{-\Delta\Delta C}t$) was obtained by normalizing to endogenous reference (18S) and in relation to a calibrator (untransfected sample).

IP-EMSA. Immunoprecipitation-electrophoretic mobility shift assay (IP-EMSA) of cytoplasmic and nuclear A549 extracts was described previously (7, 22). One milligram of protein from uninfected or RSV-infected cells was adjusted to final concentrations of 100 mM NaCl and 1% NP-40. The extract was precleared with normal rabbit serum and protein A-Sepharose for 1 h at 4°C. The supernatant was incubated overnight at 4°C with affinity-purified rabbit polyclonal antibodies to either human Bcl-3 (reactive with amino acids 290 to 421; Upstate Biotechnology, Lake Placid, NY), p50 (reactive with amino acids 350 to 363; Santa Cruz Biotechnology), or IκB-α (reactive with amino acids 297 to 317; Santa Cruz Biotechnology) and protein A-Sepharose. The immunoprecipitates were collected by centrifugation at 6,000 rpm for 1 min at 4°C and washed five times with wash buffer (20 mM HEPES, pH 7.9, 100 mM KCl, 0.2 mM EDTA, 20% glycerol, 0.5 mM phyenylmethylsulfonyl fluoride, 0.5 mM dithiothreitol) containing 1% NP-40 and once with wash buffer alone. The complexes were eluted from beads with 100 μl of 1.6% sodium deoxycholate in wash buffer for 15 min on ice. The sodium deoxycholate was neutralized with 12 μl of 10% NP-40, and the supernatant was directly used for EMSA.

EMSA for NF-κB binding was performed as described previously (23). The duplex oligonucleotide corresponding to nucleotides −96 to −69 of the human IL-8 gene promoter (sense, 5′-GATCCATCAGTTGCAAATCGTGGAATTTC CTCTCTA-3′; antisense, 5′-GATCTAGAGAGGAAATTCCACGATTTGCA ACTGATG-3′) was labeled with [α-^{32}P]dATP by Klenow fill-in reaction and used as a probe. Ten microliters of eluted sample was incubated with 1 μg of poly(dA-dT) and 50,000 cpm of ^{32}P-labeled duplex oligonucleotide in binding buffer for 15 min at room temperature. The reaction mixture was fractionated by 6% nondenaturing polyacrylamide gel, dried, and exposed to Kodak X-AR film at −70°C.

ChIP assays. The ChIP assay was performed as described elsewhere, with modifications (31, 52). On the day prior to the experiment, 2×10^6 to 4×10^6 cells were plated in medium containing 0.5% bovine serum albumin and sequentially cross-linked with disuccinimidyl glutarate (Pierce) and 1% formaldehyde in serum-free medium. The cells were washed, transferred to Eppendorf tubes, and solubilized in 400 μl of SDS lysis buffer (1% SDS, 10 mM Tris, pH 8.0, 1 mM EDTA) with protease inhibitor cocktail (Sigma Aldrich). The samples were sonicated three times for 15 s at setting 2 (Branson Sonifier 150) until DNA fragments were 300 to 400 bp or less. Equal amounts of DNA were immunoprecipitated overnight at 4°C in ChIP dilution buffer (50 mM NaCl, 1 mM HEPES, pH 7.4, 1% IGEPAL-630, 10% glycerol, 1 mM dithiothreitol) with 5 μg of either anti-HDAC-1 or IgG as indicated. Immunoprecipitates were collected with protein A-magnetic beads (Dynal, Inc.) and washed sequentially with ChIP dilution buffer, high-salt buffer (500 mM NaCl, 0.1% SDS, 1% IGEPAL-630, 2 mM EDTA, 20 mM Tris-Cl, pH 8.0), LiCl buffer (0.25 M LiCl, 1% IGEPAL-630, 1% deoxycholate, 1 mM EDTA, 10 mM Tris-HCl, pH 8.0), and TE buffer (10 mM Tris, pH 8.0, 1 mM EDTA). DNA was eluted in 1 ml of elution buffer (1% SDS in 0.1 M $NaHCO_3$). Samples were de-cross-linked in 100 mM NaCl at 65°C for 1 h. DNA was phenol extracted, ethanol precipitated, and used as template in PCR (denaturation, 94°C for 180 s; 35 cycles of 94°C for 45 s, 60°C for 60 s, and 68°C for 60 s). Primers for the IL-8 promoter were 5′-GTTGTAGTATGC CCCTAAGAG-3′ (sense) and 5′-ACACACAGTGAGAATGGTTCC-3′ (antisense). The PCR products were fractionated by agarose gel chromatography and stained with ethidium bromide.

siRNA-mediated Bcl-3 downregulation. Synthetic double-stranded Bcl-3 siRNA and nonspecific siRNA (NS siRNA) were commercially obtained (Dharmacon SMART pool, catalog no. M-003874-00). A549 cells (2.5×10^6/plate) were seeded in 6-cm tissue culture plates 1 day prior to transfection. On the day of transfection, medium was replaced with 2 ml of fresh F-12K medium containing 10% fetal bovine serum. Bcl-3 siRNA or NS siRNA was mixed with TransIT-TKO (Mirus) in OPTI-MEM according to the manufacturer's protocol and transfected into A549 cells. Cells were infected with RSV (MOI, 1:0) for 18 h. For Northern blotting, cells were harvested 48 h after transfection. For Western blotting, RSV-infected cells were harvested 72 h later.

RESULTS

Previously we have shown that RSV induces IL-8 expression in alveolar type II-like epithelial cells through an NF-κB-dependent mechanism, because inhibition of the canonical NF-κB pathway completely blocks IL-8 expression and mutation of the NF-κB binding site renders the promoter inert to RSV-induced activation (17, 51). We have found RSV infection of A549 cells results in a transient transcriptional induction, with a ~15-fold enhancement of hIL-8/LUC promoter activity by 15 h (relative to zero h) and falls thereafter, with a ~50% reduction (relative to 15 h) by 24 h and a further decrease by 36 h (Fig. 1A). The mechanism underlying the decline in IL-8 transcription is unexplained because NF-κB RelA is abundantly present in the nucleus (Fig. 1A, inset), NF-κB binding activity is increasing between 12 and 24 h after viral infection (51), and the major IκB family members (IκBα and -β) are undetectable at these time points (23). Since we have shown that the ankyrin repeat-containing Bcl-3 is involved in modulating NF-κB1 abundance in TNF-stimulated hepatic cells (7), we asked whether Bcl-3 was virus inducible and whether it may play a role in the transcriptional attenuation. A549 cells harvested at various times after RSV infection were fractionated into cytoplasmic and sucrose cushion-purified nuclear extracts and assayed for steady-state changes in Bcl-3 protein abundance by Western blotting. In control A549 cells, a specific ~56-kDa Bcl-3 band was identified to be of equal relative abundance (optical density at 595 nm of Bcl-3 signal/μg protein) in both cytoplasmic and nuclear fractions (Fig. 1B). Although Bcl-3 was thought to be a nuclear protein in B cells (61), we have previously shown that Bcl-3 is also a cytoplasmic protein in epithelial cells (7). Northern blotting for Bcl-3 transcript showed RSV-induced expression of a single 1.8-kb transcript to 3.2-fold, 3 and 6 h after RSV infection, indicating RSV-induced Bcl-3 expression through enhanced gene expression (data not shown).

We then compared Bcl-3 protein expression in control and

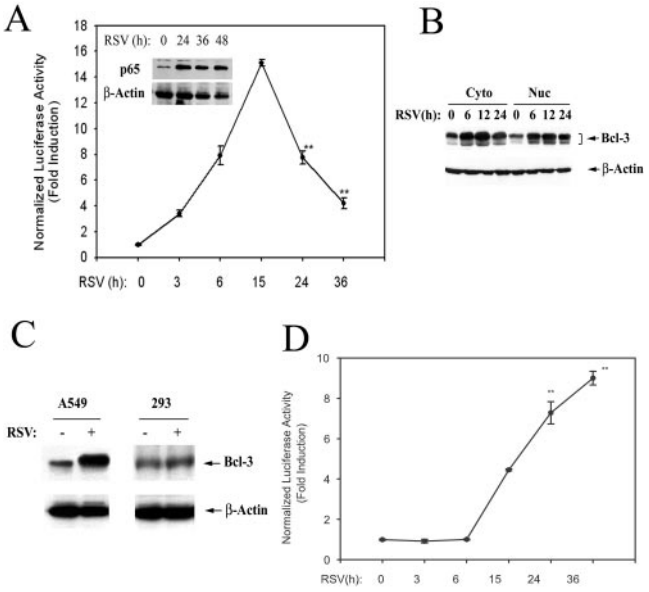

FIG. 1. Kinetics of IL-8 promoter activation in A549 cells by RSV is distinct from that of 293 cells. (A) RSV infection induces IL-8 promoter activity in A549 cells in a biphasic manner. A549 cells were transiently transfected with hIL-8 LUC (2 μg) and β-Gal (0.5 μg) plasmids. After 24 h of transfection, cells were infected with RSV (MOI, 1.0) for the indicated times, and reporter activity was measured. Luciferase activity was normalized with β-galactosidase activity and expressed as fold induction relative to zero h. Each bar is the mean ± standard error of the mean (SEM) of luciferase activity measured in triplicate from a representative experiment repeated three times. **, $P < 0.001$ from 15-h RSV infection, Student's t test. Inset, Western immunoblot for nuclear NF-κB/RelA(p65). (Bottom panel) The blot was probed with β-actin as loading control. (B) RSV infection increases Bcl-3 expression in A549 cells. A 100-μg aliquot of cytoplasmic (Cyto) and nuclear (Nuc) protein from A549 cells infected with RSV for different hours (indicated at top) was fractionated by SDS-PAGE. (Top panel) Bcl-3 was detected by Western immunoblotting. (Bottom panel) The blot was probed with anti-β-actin Ab to show equal protein loading. (C) Bcl-3 expression in RSV-infected 293 cells. Whole-cell extract was prepared from A549 and 293 cells either uninfected or infected with RSV for 15 h. Equal amounts of protein (100 μg) from A549 and 293 cell extracts were fractionated by SDS-PAGE, and Bcl-3 was detected by Western immunoblotting. (Bottom panel) β-Actin stain for loading control. (D) Kinetics of RSV-induced IL-8 promoter activity in 293 cells. 293 cells were transiently transfected with hIL-8/LUC (2 μg) and β-Gal (0.5 μg) plasmids. Cells were infected with RSV (MOI, 1.0) for the indicated times, and luciferase activity was measured 48 h after transfection. Each bar is the mean ± SEM of luciferase activity of triplicate measurements from a representative experiment repeated three times. **, significant difference from 15 h ($P < 0.001$).

RSV-infected human embryonic kidney cells (293 cells). As seen in Fig. 1C, relative to A549, the endogenous Bcl-3 levels are low in 293 cells and are not further up-regulated by RSV infection, indicating 293 cells are relatively Bcl-3 deficient. To suggest whether Bcl-3 expression may be involved in the phenomenon of transcriptional inhibition, we measured the IL-8 transcriptional profile in 293 cells in response to RSV infection. Surprisingly, we found that in contrast to the biphasic behavior of A549 cells, RSV infection induced hIL-8/LUC activity in a monotonically increasing pattern over 36 h, without attenuation (Fig. 1D). This finding identified a Bcl-3-deficient cell line to examine its effects on virus-inducible gene expression and suggested that Bcl-3 may be involved in transcriptional attenuation of NF-κB-dependent gene expression.

Bcl-3 inhibits IL-8 transcription on the NF-κB and IRF binding *cis* elements. The consequence of Bcl-3 expression on the RSV-induced IL-8 transcriptional activity was first determined by Bcl-3 coexpression in transient transfections. In 293 cells, ectopic expression of Bcl-3 can be detected by Western immunoblotting, where it is equally distributed in the cytoplasmic and nuclear fractions (Fig. 2A). To determine if ectopic Bcl-3 affected RSV-inducible IL-8 transcription, the IL-8 promoter was cotransfected in the presence of increasing concentrations of either empty vector or that encoding Bcl-3. In this experiment, RSV infection induced IL-8 promoter activity ~100-fold, and cotransfected empty vector had a small, but not statistically significant, induction compared to RSV alone (Fig. 2A). In contrast, cotransfection of vector encoding Bcl-3 reduced IL-8 promoter activity by ~50% (Fig. 2A). To determine whether Bcl-3 expression nonspecifically inhibits promoter activity, we tested the effect of increasing amounts of Bcl-3 expression on the constitutive simian virus 40 (SV40) early region promoter, where it had no inhibitory effect (data not shown). These data indicated that Bcl-3 was a potent and selective inhibitor of virus-induced chemokine transcription.

Because IL-8 is regulated by RSV on three inducible *cis* regulatory elements corresponding to the NF-κB, IRF-1, and AP-1 binding sites (9), we sought to determine which element was the major site for Bcl-3-mediated inhibition. Cells transfected with reporter genes driven selectively by NF-κB, IRF-1 (ISRE), or AP-1 binding sites in the absence or presence of Bcl-3 expression vector were then stimulated with potent agonists of each pathway (TNF for NF-κB, RSV for ISRE, and PMA for AP-1), and luciferase activity was measured. Because the level of induction varied as a function of the stimulus, to more fairly compare the inhibitory profiles the maximal stimulated reporter activity for each multimer was set to 100%. As seen in Fig. 2B, Bcl-3 inhibited the NF-κB multimer to 35% of its maximal activity, whereas it inhibited AP-1 activity only slightly, to ~80% of its maximal activity. Surprisingly, we found that the ISRE multimer was also potently inhibited, where less than 10% of its maximal activity was produced in the presence of Bcl-3. To exclude the possibility that Bcl-3-mediated inhibition was an artifact of 293 cell transformation, we examined its effect on ISRE-driven luciferase activity in HEp-2 epithelial cells (Fig. 2C). RSV infection increased luciferase activity ~15-fold over basal; consistently, Bcl-3 coexpression inhibited this activity to 50%, indicating that the Bcl-3 inhibitory effect is not unique to 293 cells.

Bcl-3 inhibits the STAT/IRF pathway. The potent effect of Bcl-3 on ISRE activity suggested that it was inhibitory for IRF-1 expression. To confirm this effect, the effect of Bcl-3 on RSV-induced native IRF-1 promoter transcription was examined. In comparison to empty vector, which had no effect on IRF-1 promoter activity, as little as 25 ng of Bcl-3 expression vector completely inhibited IRF-1 promoter activity (Fig. 3A). Because the IRF-1 promoter is itself regulated by NF-κB (34), inferring whether Bcl-3 inhibited other regulator sites in the native promoter is difficult. However, we suspected that Bcl-3 was affecting a regulatory site other than the NF-κB binding site, because Bcl-3 more potently inhibited IRF- and ISRE-dependent transcription than it did NF-κB (compare Fig. 3A

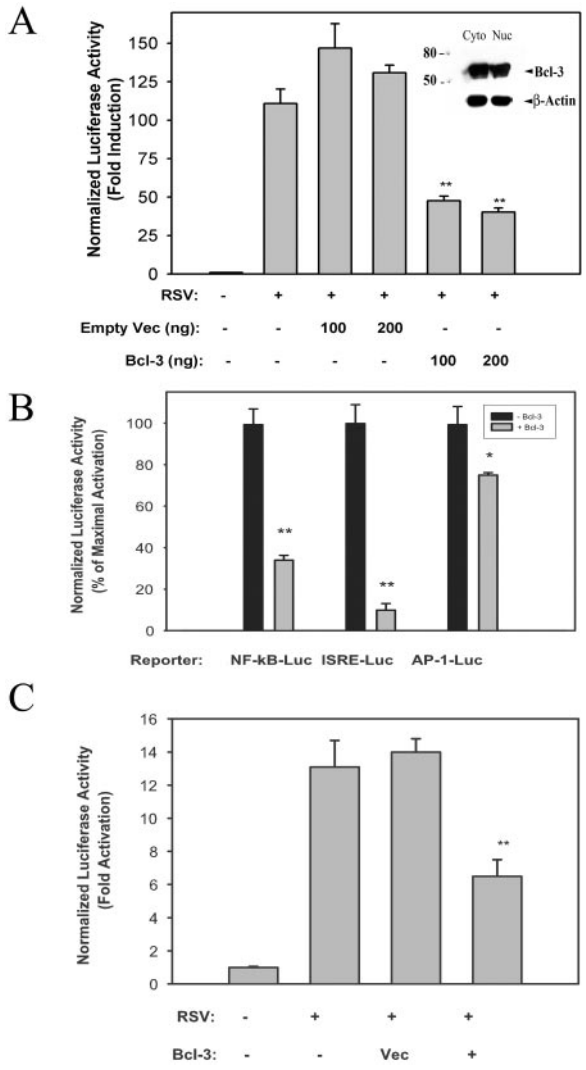

FIG. 2. Bcl-3 expression inhibits IL-8 promoter activity mediated by NF-κB and ISRE. (A) Bcl-3 inhibits RSV-induced IL-8 promoter activity. 293 cells were transfected with hIL-8/LUC reporter plasmid, pcDNA3 empty vector, or pcDNA3-Flag-Bcl-3 expression vectors as indicated. At 24 h later, cells were infected with or without purified RSV (MOI, 1.0) for 24 h, and luciferase reporter activity was measured. Luciferase reporter activity was normalized with an internal control (β-Gal activity) and expressed as the fold induction over the basal activity. Inset, Western immunoblot of cells fractionated into cytoplasmic and nuclear fractions. Molecular mass markers (in kDa) are shown at the left. Top panel, extracts were probed with anti-Flag antibody. Bottom panel, anti-β-actin Ab was used as an internal control. (B) Effect of Bcl-3 on promoter activity driven by NF-κB, ISRE, and AP-1 sites. Luciferase reporters driven by multimeric NF-κB, IRF-1(ISRE), or AP-1 sites were cotransfected with 200 ng empty vector (-Bcl-3) or Bcl-3 expression vector (+ Bcl-3) into 293 cells. Transfected cells were stimulated with TNF-α (20 ng/ml, 5 h), RSV- (MOI, 1.0, 24 h), or PMA (0.5 μM, 5 h), and luciferase reporter activity was measured. Luciferase activity was normalized with β-Gal activity. Relative to unstimulated controls, TNF stimulated the NF-κB multimer 200-fold, RSV induced the ISRE multimer 140-fold, and PMA induced the AP-1 multimer by 50-fold. Data are represented as the percentage of maximal reporter activity (set at 100%). Each bar is the mean ± standard error of the mean (SEM) of two experiments done in triplicate. *, $P < 0.05$; **, $P < 0.001$; Student's t test. (C) Bcl-3 inhibits ISRE-driven transcriptional activity in HEp-2 cells. HEp-2 cells were transiently cotransfected with 2 μg (ISRE)x3-Luc plasmids and pcDNA3-Flag-Bcl-3 (Bcl-3) or empty vector (Vec) (100 ng). After 24 h, transfected cells were infected with RSV for 24 h and luciferase activity was measured. Results are means ± SEM of two experiments with triplicate deattenuations. Luciferase activity was normalized with β-Gal activity and is expressed as the fold activation over uninfected cells. **, significantly different from RSV-infected cells ($P < 0.001$).

and 2B). Previous work has shown that STAT-1 and -3 binding plays an important regulatory role in inducible IRF-1 gene expression (34). To determine whether Bcl-3 also affected the STAT pathway, its effects on STAT-dependent reporter activity were studied in response to pathway activation mediated by the Jak/Tyk tyrosine kinases (IL-6 and IFN-γ) or that mediated by tyrosine phosphatase inhibition (RSV infection [11]). Bcl-3 inhibited reporter activity by all agonists, indicating that its effect was stimulus type independent (Fig. 3B). To further demonstrate the potent effect of Bcl-3 on the activity of the STAT pathway, the Bcl-3 inhibitory dose-response profile was determined. Here, increasing concentrations of Bcl-3 expression vector were cotransfected with each of the selective multimeric reporter plasmids. Bcl-3 inhibited the IL-6-induced STAT reporter by >50% at the lowest concentration of expression plasmid (12.5 ng) (Fig. 3C), whereas 50% inhibition of the NF-κB-dependent promoter was not observed until 50 to 100 ng of expression plasmid. These results showed that Bcl-3 was a potent inhibitor of both the NF-κB and the STAT/IRF pathways. We next investigate the interaction of Bcl-3 with NF-κB, but we will then return to the more novel finding of its effect on the STAT/IRF pathway.

RSV induces nuclear Bcl-3–NF-κB association. We have previously shown that NF-κB binding is increased at 12 to 24 h, during the time at which the transcriptional shut-off is occurring. However, this is apparently inconsistent with the previously reported activity of Bcl-3 to recapture NF-κB1 into the cytoplasm (7). We therefore determined whether Bcl-3 associated with NF-κB in the nucleus and if this association was regulated by RSV infection. Control or RSV-infected A549 nuclear extracts (NE) were subjected to IP-EMSA (7). In this technique, NE was immunoprecipitated with anti-Bcl-3 or anti-IκBα antibodies. After gentle dissociation of the immune complexes, EMSA was used to detect NF-κB binding activity. We have previously shown that this detection of NF-κB binding activity was dependent on the primary antibody used in the immunoprecipitation reaction, an observation that excluded nonspecific binding of NF-κB complexes to protein A beads (7). In control extracts, anti-Bcl-3 antibody precipitated a predominant high-mobility complex (C1) (Fig. 4A). In NE from cells RSV infected for 24 h, an increase in binding of C1 complex was seen, and the presence of several lower-mobility complexes (C2 and C3) was also observed. Linearity of the assay with respect to input protein was determined in parallel using different amounts of NE from RSV-infected cells corresponding to 0.5 and 2.0 mg protein (Fig. 4B, right panel). Together these data indicated that the abundance of NF-κB-associated Bcl-3 in the nuclear fraction increased approximately fourfold after RSV infection. A similar C1 complex was also formed when cytoplasmic extract from uninfected cells was immunoprecipitated with IκBα antibody, but we noted subtle differences in the pattern of slower-migrating C2 and C3 complexes compared to that produced by anti-Bcl-3 (Fig. 4A,

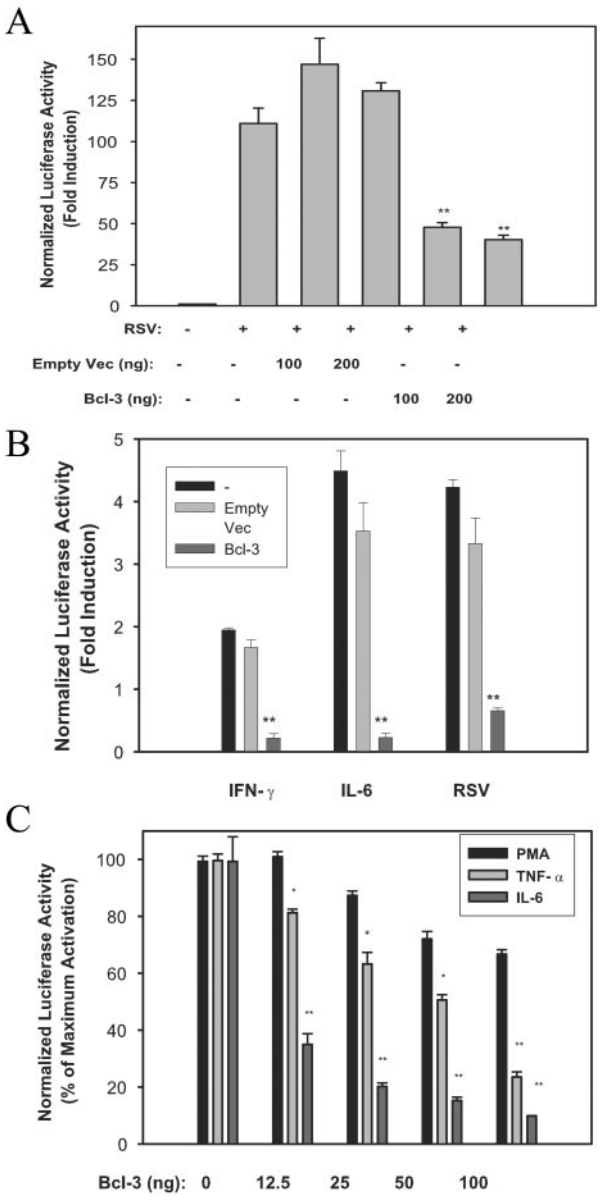

FIG. 3. Bcl-3 expression inhibits the STAT/IRF-1 pathway. (A) Bcl-3 inhibits IRF-1 promoter activity. A549 cells were cotransfected with 2 μg hIRF-1/LUC plasmids and either pcDNA3-Flag-Bcl-3 (Bcl-3) or empty vector (Vec). Where indicated, cells were infected with RSV (MOI, 1.0; 24 h). Shown is the normalized luciferase reporter activity. (B) Stimulus type-independent inhibition of STAT-Luc by Bcl-3. 293 cells were transiently transfected with STAT-Luc reporter plasmid with or without Bcl-3 expression vector. Following 24 h of transfection cells were either left untreated (-) or treated with IFN-γ, IL-6, or RSV for 24 h. Each bar is the mean ± standard error of the mean (SEM) of a representative experiment repeated twice. **, significant difference from IFN-γ, IL-6, or RSV alone ($P < 0.001$). (C) Bcl-3 is a highly potent inhibitor of STAT activity. 293 cells were transfected with STAT-Luc, NF-κB-Luc, or AP-1-Luc and either cotransfected with empty vector or an increasing amount of Bcl-3 expression vector (Bcl-3), and luciferase activity was measured following IL-6 (24 h), TNF (6 h), or PMA (5 h) stimulation. Data are means ± SEM of a representative experiment with triplicate deattenuations. *, $P < 0.05$ from RSV alone; **, $P < 0.001$ from RSV alone.

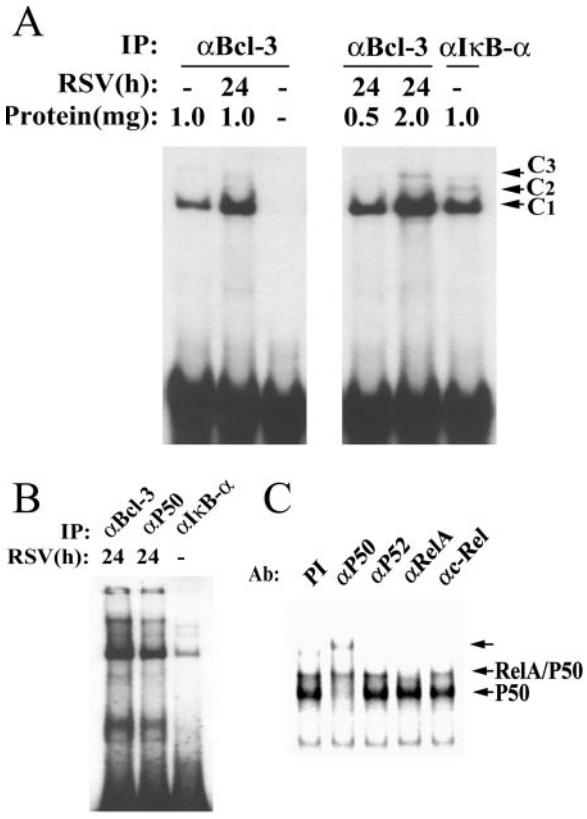

FIG. 4. Bcl-3 inhibits NF-κB-dependent IL-8 transcription through NF-κB association. (A) RSV infection increases Bcl-3 association with NF-κB. Immunoprecipitation (IP)-EMSA was done with nuclear extract from uninfected or RSV-infected A549 cells. Nuclear protein (0.5, 1, and 2 mg) was IP with ant-Bcl-3 Ab (αBcl-3) or anti-IκB-α Ab (αIκB-α), dissociated from beads, and used in an EMSA performed with ^{32}P-labeled double-stranded NF-κB binding site from the IL-8 promoter (see Materials and Methods). (B) NF-κB complex associated with IκBα is distinct from that associated with Bcl-3. Nuclear protein (1 mg) from RSV-infected A549 cells was IP with anti-Bcl-3 Ab (αBcl-3) or anti-p50 Ab (αp50). Cytoplasmic protein (1 mg) from uninfected cells was immunoprecipitated with anti-IκBα antibody (αIκBα). The NF-κB site was analyzed by EMSA, as in Fig. 3B. (C) Identification NF-κB subunits by antibody supershift assay. Nuclear proteins obtained by IP using anti-Bcl-3 Ab were incubated with preimmune serum (PI) or antibody to p50, p52, p65, or cRel on ice for 30 min prior to EMSA. The compositions of the DNA binding complex and the supershifted band were indicated by the arrow on the right.

right panel). To determine if Bcl-3-associated complexes were similar to the NF-κB1 species, the EMSA binding patterns for complexes from RSV-infected cells were compared for Bcl-3, NF-κB1, and IκBα (Fig. 4B). The binding patterns of proteins associated with Bcl-3 and NF-κB1 were indistinguishable and slightly different from those cytoplasmic proteins associated with IκBα (Fig. 4B). In binding competition experiments, all three complexes were competed specifically by the wild-type (WT) but not by the mutated duplex oligonucleotide (data not shown). To establish the subunits of NF-κB complexes associated with Bcl-3, a panel of subunit-specific affinity-purified antibodies to different NF-κB members were used for supershift in EMSA. As shown in Fig. 4C, the higher-mobility C1 complex was completely supershifted by anti-NF-κB1, suggest-

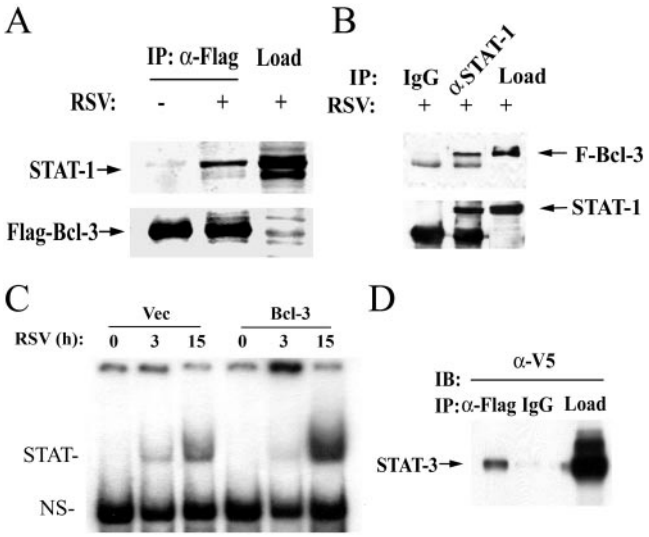

FIG. 5. Bcl-3 interacts with STAT-1 in RSV-infected nuclei. (A) Nondenaturing co-IP of Bcl-3 complexes. Bcl-3-transfected 293 cells were uninfected or infected with RSV for 20 h. A 250-μg aliquot of nuclear extract was IP with anti-Flag Ab. STAT-1 in immune complexes was detected by Western immunoblotting. Load, input sample. (Bottom panel) The membrane was reprobed with anti-Flag Ab to determine Bcl-3 recovery. (B) Nondenaturing co-IP of STAT-1 complexes. Flag-Bcl-3 expression vector (2.5 μg) was transfected into 293 cells. A 250-μg aliquot of nuclear protein was IP using anti-STAT-1 Ab (α-STAT-1) or preimmune rabbit IgG (IgG). Starting material (load) was used as staining control. (Top panel) Flag-Bcl-3 in the immune complex was detected in the Western immunoblot assay using anti-Flag Ab. (Bottom panel) STAT-1 recovery was detected by reprobing the membrane with anti-STAT-1 Ab. (C) Bcl-3 expression does not inhibit RSV-induced STAT-1 and -3 DNA binding, as shown with the EMSA of STAT DNA binding activity. 293 cells were transfected with either 2.5 μg of empty vector (Vec) or 2.5 μg pcDNA3-Flag-Bcl-3 expression vector (Bcl-3) for 24 h. Cells were then RSV infected (MOI, 1) for the indicated times, and nuclear protein was extracted. An EMSA was carried out with 15 μg protein using ^{32}P-labeled SIE probe. STAT, inducible STAT-1 and -3 binding complex; NS, nonspecific binding B. (D) Bcl-3 associates with STAT-3. V5-tagged STAT3 and Flag-Bcl-3 expression vectors were cotransfected. Lysates were immunoprecipitated with anti-Flag Ab or IgG as indicated. STAT-3 in the immune complex was detected with Western blotting using anti-V5 Ab.

ing that this complex was composed of p50 homodimers. In contrast, the lower-mobility C2 complex was primarily supershifted by anti-RelA antibody, indicating that Bcl-3 associated (directly or indirectly) with RelA. Together, these results indicate that Bcl-3 is primarily associated with NF-κB1 in the nucleus of airway epithelial cells and that this association is enhanced by RSV infection.

Bcl-3 physically associates with STAT-1 and -3. We next returned to understand the mechanism for inhibition of the STAT/IRF pathway. To determine whether endogenous STAT-1 physically associates with Bcl-3 in RSV-infected 293 cells, nondenaturing co-IP assays were performed. Nuclear extract from uninfected or RSV-infected cells expressing Flag-Bcl-3 was immunoprecipitated with anti-Flag Ab as the primary Ab, and STAT-1 was detected by Western immunoblotting (Fig. 5A). Although equivalent amounts of Flag-Bcl-3 were recovered, RSV induced a strong STAT-1 signal. These results showed that RSV infection dramatically increased Flag-Bcl-3 association with STAT-1 in the nucleus. To validate this finding and control for nonspecific effects, the converse experiment was performed in RSV-infected cells where nuclear extract was immunoprecipitated with either IgG or anti-STAT-1 Ab. The presence of STAT-1 and Bcl-3 was then detected by Western immunoblotting. Anti-STAT-1 Ab specifically immunoprecipitated endogenous STAT-1, because this band was not observed in extracts precipitated with nonimmune IgG (Fig. 5B, lower panel). Importantly, a specific Bcl-3 band was found only in the STAT-1 immunoprecipitate (Fig. 5B, upper panel). To determine whether Bcl-3 affected STAT binding, 293 cells were transiently transfected with empty or pcDNA-Flag-Bcl-3 expression vector. Cells were RSV infected, and nuclear extract was subjected to EMSA using the high-affinity STAT SIE binding site (Fig. 5C). In the presence of cotransfected Bcl-3, we observed that RSV induced enhanced, not reduced, binding of the STAT-1 and -3 isoforms. Finally, to determine whether Bcl-3 specifically associated with STAT family members, a co-IP assay was performed to detect association with STAT-3. As seen in Fig. 5D, co-IP also showed that Bcl-3 interacts with STAT-3.

Bcl-3 increases HDAC-1 recruitment on the IL-8 promoter. We observed that although Bcl-3 interacted with STAT-1 and inhibited STAT-dependent transcription, it did not inhibit its DNA binding. Therefore, we examined if a transcriptional repressor were involved in this effect. Recently, it has been shown that Bcl-3 inhibits lipopolysaccharide-stimulated TNF-α expression in macrophages through association with HDAC-1 (56). By virtue of its ability to deacetylate histones and transcription factors, HDAC-1 is an inhibitor of both NF-κB1- and IL-6-induced STAT3-dependent transcription (56). We therefore examined the association of endogenous Bcl-3 and HDAC-1 in A549 cells following RSV infection by nondenaturing co-IP. Nuclear extracts from uninfected or RSV-infected A549 cells were immunoprecipitated with anti-Bcl-3 antibody, and the presence of HDAC-1 was determined by Western immunoblotting (Fig. 6A). Here, we observed that nuclear Bcl-3 strongly associated with HDAC-1.

To examine whether Bcl-3 and HDAC-1 inducibly bind the native IL-8 promoter, a time course of RSV infection in A549 cells was examined by ChIP assay. Chromatin was cross-linked after various times of RSV infection and immunoprecipitated with anti-Bcl-3 Ab or anti-HDAC-1 Ab (Fig. 6B). We observed that Bcl-3 binding, undetectable in uninfected cells, was induced 15 h after RSV infection, peaking after 24 h of infection. Similarly, HDAC-1 binding showed a similar induction pattern, with peak binding 24 h after infection, a time at which IL-8 gene transcription was falling (cf. Fig. 1A). Together, these data indicate that Bcl-3 and HDAC-1 are targeted to the native IL-8 promoter in response to RSV infection.

We next asked whether Bcl-3 expression enhanced HDAC-1 binding to the IL-8 promoter. 293 cells were transfected with empty or Bcl-3 expression vectors, and a ChIP assay was performed using anti-HDAC-1 Ab. IP with preimmune serum (IgG) did not capture significant amounts of the IL-8 promoter; however, IP with anti-HDAC-1 Ab produced a weak IL-8 PCR product (Fig. 6C). By contrast, in Bcl-3-expressing cells, the amount of HDAC-1-associated IL-8 was significantly increased (Fig. 6C, lanes 2 and 3). These results clearly showed

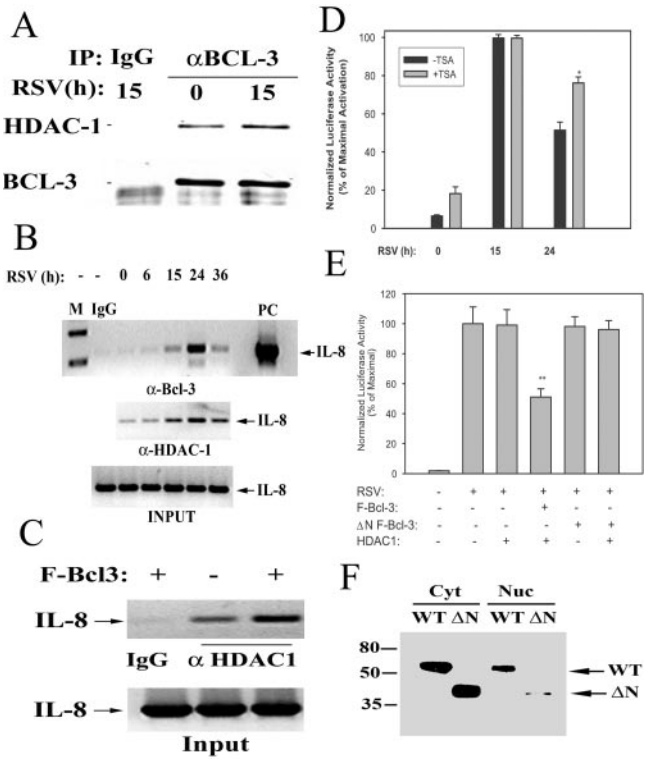

FIG. 6. Bcl-3 recruits HDAC-1 to the IL-8 promoter. (A) RSV infection increases Bcl-3 and HDAC-1 association in vivo. Nuclear extracts (1 mg) from control or RSV-infected (15 h) A549 cells were IP with anti-Bcl-3 Ab (α-BCL-3) or IgG. Immune complexes were washed, and HDAC-1 was detected by Western immunoblotting. (Bottom panel) The membrane was reprobed with anti-Bcl-3 Ab. (B) HDAC-1 and Bcl-3 recruitment to the IL-8 promoter in RSV infection, as shown in a ChIP assay with A549 cells infected with RSV for the times indicated. Shown is ethidium bromide-stained agarose gel. (Top panel) IL-8 promoter PCR of chromatin IP with IgG or anti-Bcl-3 Ab (α-Bcl-3). (Middle panel) PCR of chromatin IP with anti-HDAC-1 Ab. Bottom panel, control PCR for equivalent amount of DNA used as input for IP (input). M, DNA size markers; PC, positive control genomic DNA. (C) Bcl-3 expression enhances HDAC-1 recruitment to IL-8 promoter. Empty pcDNA (-) or Flag-Bcl-3 expression vectors (+) were transfected into 293 cells. After 24 h, a ChIP assay was performed using either anti-HDAC-1 Ab (α-HDAC-1; 5 μg; lanes 2 and 3) or IgG (lane 1) as described in Materials and Methods. (Upper panel) IL-8 PCR of HDAC-1 IP chromatin; (lower panel) IL-8 PCR from IP input. (D) An HDAC inhibitor reverses late-phase IL-8 inhibition. A549 cells were transfected with hIL-8/LUC. After 24 h, cells were pretreated with or without TSA (100 nM) for 5 h and infected with RSV for the indicated times. Luciferase activity was normalized with β-galactosidase activity and expressed as the percentage of maximal activation observed at 15 h of RSV infection. *, $P < 0.01$ at same infection time, +TSA versus –TSA; **, $P < 0.001$ compared to RSV infection alone. (E) HDAC-1 inhibition of transcription requires nuclear Bcl-3. 293 cells were transfected with 0.5 μg ISRE-Luc or cotransfected with 500 ng of HDAC-1, 200 ng of WT Flag-Bcl-3, or N-terminal deletion mutant (ΔN Flag-Bcl-3) plasmids as indicated. After infection with RSV for 24 h, cells were lysed and luciferase activity was measured. Each bar is the mean ± standard error of the mean of normalized luciferase activity from two experiments done in triplicate. (F) Wild-type but not the N-terminal deletion mutant of Bcl-3 is localized in the nucleus. 293 cells were transiently transfected with 2.5 μg of WT or the N-terminal deletion (ΔN) of Flag-tagged Bcl-3 plasmids. After 24 h, cytoplasmic (Cyt) and nuclear (Nuc) extracts were prepared from the transfected cells as described in Materials and Methods. WT or ΔN Flag Bcl-3 was detected by Western immunoblotting using Flag monoclonal antibody. Numbers on the left indicate molecular weight standards.

that Bcl-3 expression increased HDAC-1 recruitment to the endogenous IL-8 promoter.

Earlier we found that IL-8 promoter activity is inhibited to ~50% in A549 cells 24 h after RSV infection (Fig. 1A). Hypothesizing that this inhibition might be due to HDAC recruitment, we asked if TSA, a potent inhibitor of HDACs, could reverse this attenuation of promoter activity. A549 cells transiently transfected with the hIL-8/LUC reporter were pretreated with or without TSA (100 nM) prior to RSV infection. As shown in Fig. 6D, RSV infection again produced a biphasic profile of hIL-8/LUC reporter activity. We noted that TSA pretreatment partially reversed this inhibitory effect of RSV infection at the 24-h time point. These results indicated that late-phase attenuation of IL-8 transcription is (at least partially) mediated by HDACs in A549 cells.

To determine whether HDAC-1-mediated repression is Bcl-3 dependent, we infected 293 cells transiently transfected with ISRE-Luc reporter plasmids and HDAC-1 in the absence or presence of Bcl-3 expression vector. As shown in Fig. 6E, HDAC-1 did not inhibit luciferase activity, except in the presence of full-length WT Flag-Bcl-3. To determine whether nuclear Bcl-3 was required for the inhibition mediated by HDAC-1, 293 cells were cotransfected with an NH_2-terminal deletion of Bcl-3 (ΔN Flag-Bcl-3), previously shown to be deficient in nuclear translocation (25). Nuclear extracts from transiently transfected cells were prepared by our published sucrose cushion method, which produces nuclear proteins free of cytoplasmic protein contamination (7, 8). In comparison to full-length Bcl-3, although ΔN Flag-Bcl-3 was expressed 1.3-fold higher but only 1.7% was nuclear, 10% of full-length Bcl-3 was nuclear (Fig. 6F). Importantly, HDAC-1 was not able to inhibit IL-8 transcription in the presence of the nuclear localization-deficient Bcl-3 (Fig. 6E, right columns). These results clearly show that HDAC-1 recruitment on the IL-8 promoter is Bcl-3 dependent and requires its nuclear targeting.

Bcl-3 down-regulation up-regulates chemokine expression in RSV-infected A549 cells. We have observed that Bcl-3 coexpression in transiently transfected 293 and Hep2 cells inhibited chemokine promoter activity in a stimulus type-independent manner (Fig. 2 and 4). To exclude a transient-transfection artifact, endogenous chemokine expression was measured in A549 cells after siRNA-mediated Bcl-3 knockdown. Bcl-3 expression in A549 cells transfected with Bcl-3-specific siRNA was first measured by both Northern and Western blotting. From results not shown, 50 nM Bcl-3 siRNA inhibited steady-state Bcl-3 mRNA levels by ~50% (relative to control) in both uninfected and RSV-infected cells. Conversely, NS-siRNA had no significant effect on Bcl-3 expression. Similarly, 50 nM Bcl-3 siRNA reduced Bcl-3 protein levels to less than uninduced control without affecting β-actin expression (Fig. 7A). We then examined the effect of Bcl-3 down-regulation on IL-8 and IRF-1 expression by RSV-infected A549 cells by Q-RT-PCR. As shown in Fig. 7B (top panel), RSV induced IL-8 mRNA expression ~4-fold in untransfected cells and slightly less in NS-siRNA-treated cells. In contrast, RSV infection increased IL-8 expression ~7-fold in Bcl-3 siRNA-treated cells. Similar qualitative findings were observed with RSV-induced IRF-1 expression. Together, these results clearly indicate that indeed RSV-induced Bcl-3 induction plays a negative regulatory role in the late-phase chemokine expression.

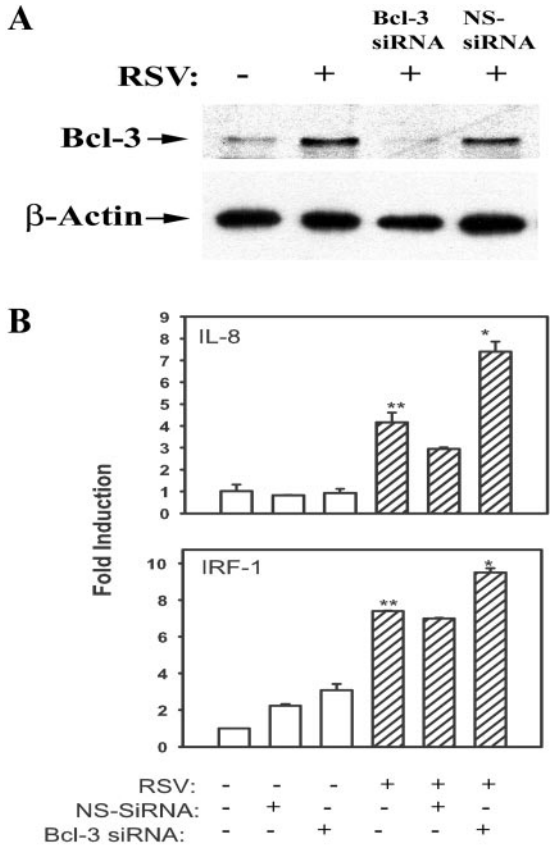

FIG. 7. siRNA-mediated down-regulation of endogenous Bcl-3 enhances RSV-induced IL-8 and IRF-1 expression in A549 cells. (A) Down-regulation of Bcl-3 protein expression. (Top panel) Whole-cell lysate (200 μg protein) from A549 cells was transfected either with Bcl-3 siRNA (50 nM) or NS-siRNA (50 nM) and was infected with (+) or without (-) RSV. Bcl-3 was detected by Western immunoblotting. (Bottom panel) The same membrane was reprobed with anti-β-actin Ab to show equal loading. (B) Bcl-3 down-regulation enhances RSV-induced IL-8 and IRF-1 expression. RNA from untransfected NS-siRNA (50 nM) or Bcl-3 siRNA (50 nM) cells with or without RSV infection was subjected to Q-RT-PCR. (Top panel) IL-8 transcript levels; (bottom panel) IRF-1 mRNA. All data presented are normalized to 18S RNA and expressed as the fold induction relative to untransfected and uninfected controls. Results are means ± standard deviations of two experiments run in duplicate. *, $P < 0.02$; **, $P < 0.001$.

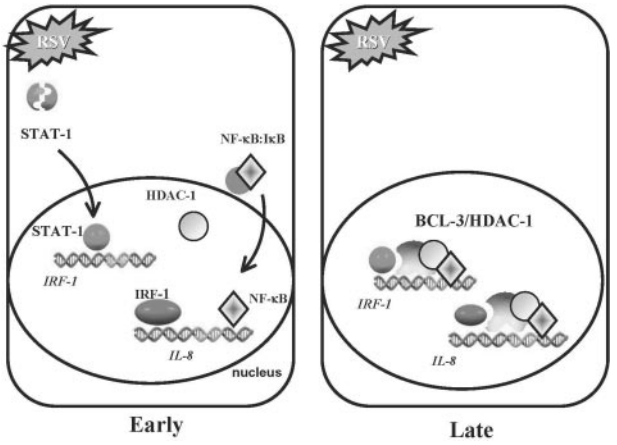

FIG. 8. Schematic model for Bcl-3-mediated inhibition of chemokine expression. Based on these findings, Bcl-3 inhibits RSV-induced chemokine expression by antagonizing the NF-κB and STAT-1/IRF signaling pathways. Shown is a schematic diagram of activated nuclear factors early (left) in the course of RSV infection (<12 h), and late (right) in the course of RSV infection (>24 h). Early in the course of RSV infection, the IL-8 promoter is occupied by transcription factors corresponding to the IRF-, STAT, and NF-κB families (for simplicity, only IRF-1 and STAT-1 are depicted), and IRF-1 synthesis is STAT-1 dependent. Late in the course of RSV infection, Bcl-3 is synthesized, where it antagonizes the transcriptional activity of NF-κB and STAT-1 by complexing and recruiting HDAC-1 to target genes.

DISCUSSION

In severe lower respiratory tract infections with RSV, RSV replication initiates mononuclear leukocytes, neutrophils, and eosinophils to be recruited into the lower respiratory tract. In isolated airway epithelial cells, RSV is a potent inducer of chemokine expression by a complex transcriptional control mechanism involving common nuclear factors, NF-κB, AP-1, and the IRF pathway. These factors work in concert to activate IL-8 gene expression by participating in a multiprotein complex termed the enhanceosome (9, 49). Although the control mechanisms governing the initial activation pathways of both the NF-κB and STAT transcription factors have been the focus of much study, it is clear that their activity is actively terminated through poorly understood mechanisms. Although the NF-κB–IκB autoregulatory loop appears to control NF-κB's nuclear action in response to cytokine and PMA stimulation in a number of cell types (7, 20, 47), this pathway does not account for attenuation of NF-κB in virally infected epithelial cells, because IκBα is undetectable after its initial proteolysis and is not resynthesized (23). In addition, attenuation of STAT transcriptional activity has largely focused on the SOCS and PIAS inhibitors (reviewed in references 2 and 57). In this study, we examined the role of the Bcl-3 protein in terminating chemokine expression. Bcl-3 is rapidly induced in RSV-infected airway cells in both the cytoplasmic and nuclear compartments of RSV-infected A549 cells, where it associates with NF-κB and inhibits its activity. Our previous work showed that Bcl-3 induction is mediated through the effect of NF-κB action (7), and it is therefore likely that Bcl-3 induction is not specific to RSV infection but may be general to all NF-κB-activating viruses. Although this work is confirmatory in indicating that Bcl-3 is an antagonist of NF-κB-dependent binding and transcription (24, 58), we have made the surprising observation that Bcl-3 is a potent inhibitor of the STAT/IRF pathway. Expression of Bcl-3 in a Bcl-3-deficient cell line blocks virus-inducible expression of IRF-1; this effect appears to be partly mediated through a STAT regulatory element as a result of Bcl-3 complexing with STAT-1. In addition, nuclear Bcl-3 complexes with HDAC-1 enhancing its recruitment to target genes binding NF-κB and STAT. We have shown that the late-phase attenuation of chemokine transcription is partially inhibited by the HDAC inhibitor TSA and, finally, down-regulation of endogenous Bcl-3 up-regulates chemokine expression in RSV-infected cells. These studies suggest that inducible Bcl-3 functions in a pleiotropic mechanism terminating virus-inducible chemokine transcription by antagonizing both the NF-κB and STAT/IRF pathways, as schematically shown in Fig. 8.

The NF-κB–IκB autoregulatory loop. Although NF-κB is an important regulator of gene networks in virus-infected epithelial cells (51), uncontrolled NF-κB activity is apparently deleterious. In response to activation by type I cytokines, such as TNF, NF-κB only transiently resides in the nucleus, being recaptured in the cytoplasm through an active protein synthesis-dependent process, the major pathway being the NF-κB–IκBα autoregulatory feedback loop (20, 21, 46). Here, NF-κB induces IκBα resynthesis through multiple NF-κB binding sites present in the IκBα promoter. As a result, within 1 h of NF-κB's nuclear appearance, IκBα protein reaccumulates, capturing RelA back into the cytoplasm through a CRM1-dependent export mechanism (48). However, in response to other stimuli, different IκB members can be induced to capture specific NF-κB family members and at different times, indicating that this autoregulation is complex. For example, Bcl-3 and IκBγ, genes induced much more slowly than IκBα, primarily associate with the DNA binding subunits NF-κB1 and -2 (7, 24, 58; reviewed in reference 28). In cytokine-stimulated HepG2 cells, we previously observed that Bcl-3 expression was inducible in an NF-κB-dependent manner, resulting in selective cytoplasmic sequestration of NF-κB1 6 to 12 h after cytokine stimulation (7). Therefore, although the induction of Bcl-3 expression was much slower than that of IκBα in the same cells, these findings were the first to suggest the existence of a second autoregulatory loop, the NF-κB–Bcl-3 loop, whose function is to sequester the NF-κB1 DNA binding subunit. This study is the first to show Bcl-3 up-regulation in human pulmonary epithelial cells following RSV infection, where it participates in NF-κB transcriptional attenuation in the absence of IκBα resynthesis. We show here that the effect of Bcl-3 is inhibitory by its ability to complex and recruit HDAC-1, in addition to its ability to sequester NF-κB1 in the cytoplasm.

A number of different agents have been shown to increase Bcl-3 expression in different cell types. For example, mitogenic stimuli (PMA, phytohemagglutinin, IL-9, granulocyte-macrophage colony-stimulating factor, and erythropoietin) increased Bcl-3 expression severalfold above the control in human B cells, T-helper cell lines, mast cells, and erythroleukemia cells (32, 36, 60). Here we have observed that viral replication is another potent inducer of Bcl-3 expression in alveolar epithelial cells. Recently studies from our group have shown that TNF-α induces Bcl-3 expression in HepG2 cells by inducing RelA to bind to a proximal NF-κB binding site in its promoter (7). Similarly, we believe the induction of Bcl-3 in virally infected epithelial cells is probably NF-κB dependent, although this will require direct experimentation.

Bcl-3 inhibits the STAT/IRF pathway. The most significant and surprising finding in our study is the potent effect of Bcl-3 on inhibiting the STAT/IRF pathway in a manner independent of stimulus type. Recently we showed that RSV infection of A549 cells activates different isoforms of STATs, including STAT-1 and -3, through tyrosine phosphorylation increasing their binding to the IRF-1 GAS site (27). We have previously shown that RSV infection induces IRF-1 expression by A549 cells. A large body of evidence suggests that IRF-1 is transcriptionally regulated through binding of NF-κB and STAT to their respective *cis* elements present in the IRF1 promoter in response to cytokine and viral infection (26, 34).

Our data suggest that nuclear Bcl-3 plays a pleiotropic role in terminating IL-8 expression through direct and indirect mechanisms (schematically diagrammed in Fig. 8). Previous work on the IL-8 regulatory elements have indicated that the IRF binding site (RSVRE) is an essential site for RSV-inducible transcription, because its deletion renders the promoter inert to viral induction (9). The expression of IRF-1, in turn, is partly controlled by STAT-1 binding to a high-affinity GAS site in its proximal promoter (26); indeed, we have found that Bcl-3 inhibits virus-inducible IRF-1 expression by interference with the upstream STAT-1 transactivator. In addition to its ability to interfere with STAT transactivation, Bcl-3 also affects NF-κB-dependent transcription directly on the IL-8 promoter, making genes such as IL-8 and IRF-1 particularly sensitive to its inhibitory effects.

Bcl-3 physically associates with STAT-1. Our coimmunoprecipitation assays suggest that STAT-1 and Bcl-3 stably interact in the cell nucleus. In addition to the observations showing the Bcl-3-STAT interaction in this report, other studies have shown that Bcl-3 interacts with other classes of transcription factors, including NF-κB, AP-1 (c-Jun and c-Fos [29]), and E4TF1/GABP (43). Interestingly, the effect of Bcl-3 on transcriptional inhibition is greatest on the STAT pathway in a stimulus-independent manner (Fig. 3B). This report is the first, to our knowledge, to demonstrate that Bcl-3 forms a stable association with STAT-1 and -3 isoforms. Bcl-3 is a 46-kDa phosphoprotein containing a proline-rich NH_2 terminus, seven cdc10-like ankyrin repeats in the center of the protein, and a proline/serine-rich COOH terminus (32). Although the ankyrin repeat domains of Bcl-3 mediate binding to NF-κB isoforms, further work will be required to identify the STAT interacting domains and to establish whether this association is direct.

Bcl-3, HDAC-1, and transcriptional inhibition. Bcl-3 has been previously shown to also associate with the CEBP/p300 and SRC1 classes of coactivators (29). In addition, Bcl-3 apparently functions as a bridging factor by promoting association between p50 and Jab1, Pirin, Tip60, and Bard1, an association that apparently induces transcriptional activity (14). In our system, Bcl-3 functions largely as a virus-induced transcriptional attenuator, indicating its function is under cell type-dependent control. As a potential mechanism, we found that HDAC-1 is another important transcriptional modulatory protein to which Bcl-3 associates. Our ChIP assays indicated that HDAC-1 association with chemokine promoters is enhanced by increasing levels of nuclear Bcl-3 (Fig. 6B). Supporting the enzymatic action of HDAC-1 in mediating transcriptional attenuation of chemokine transcription, we found that TSA partially prevents the turn-off of transcription in A549 cells (Fig. 6C). HDACs are potent transcriptional modulators, being able to reverse nucleosomal relaxation produced by histone acetylase activity contained within the CEBP/p300 P/CAF and GCN5 coactivators. It has been reported that HDAC-1 associates with the nuclear 50-kDa NF-κB1, reducing transcriptional activity of a subset of NF-κB-dependent genes (63). Our studies here suggest that Bcl-3 also inhibits the STAT pathway by HDAC-1 recruitment. In separate experiments, we have recently shown that the transcriptional actions of STAT-33 are highly inhibited by HDAC-1 (35). Here, acetylation of the STAT-33 NH_2 terminus is required for acquisition of transcriptional activity by promoting its stable association with p300/

CBP. The actions of HDAC-1 to reduce STAT acetylation would therefore reduce coactivator recruitment and target gene activity. In this manner, HDAC-1 may have inhibitory actions on target gene expression independently of its effect on chromatin structure. Also, recently it has been shown that p53-mediated Bcl-3 down-regulation results in enhanced HDAC-1 binding to NF-κB p52 and inhibition of cyclin D1 expression (37). Interpreted together with our findings, we suggest that Bcl-3 may act to target the nuclear HDAC-1 reservoir to specific genes. In the setting of viral infection, enhanced Bcl-3 expression captures free HDAC-1 and targets it to promoters containing STAT binding sites, attenuating their activity.

In summary, RSV-induced chemokine gene expression in epithelial cells is controlled by a complex pathway involving common transcription factors and regulatory molecules that interact in a promoter-specific context. Although chemokine expression is important in the host response to respiratory virus infection, redundant cellular mechanisms are activated to terminate the transcriptional activation process. Here we provide evidence that Bcl-3 induction by RSV is a feed-forward negative regulator of IL-8 expression. In addition to the well-described NF-κB–Bcl-3 autoregulatory loop, we have identified a novel mechanism of Bcl-3 action to antagonize the STAT/IRF pathway by promoting HDAC-1 recruitment to target genes. These data suggest that, in the context of viral infection, Bcl-3 serves to modify the acetylation status of histones and transcription factors on activated inflammatory chemokine promoters.

ACKNOWLEDGMENTS

This project was supported by grants from the American Heart Association (0060037Y to M.J.), NIAID (AI40218 to A.R.B.), NICHHD (R30HD 27841), and P30 ES06676 from the NIEHS (to J. Halpert, UTMB).

We gratefully acknowledge Tom Wood, Director of the UTMB Recombinant DNA lab, for plasmid construction.

REFERENCES

1. **Aherne, W. T., T. Bird, S. D. B. Court, P. S. Gardner, and J. McQuillin.** 1970. Pathological changes in virus infections of the lower respiratory tract in children. J. Clin. Pathol. **23:**7–18.
2. **Alexander, W. S., R. Starr, J. E. Fenner, C. L. Scott, E. Handman, N. S. Sprigg, J. E. Corbin, A. L. Cornish, R. Darwiche, C. M. Owczarek, T. W. Kay, N. A. Nicola, P. J. Hertzog, D. Metcalf, and D. J. Hilton.** 1999. SOCS1 is a critical inhibitor of interferon gamma signaling and prevents the potentially fatal neonatal actions of this cytokine. Cell **98:**597–608.
3. **Baggiolini, M., B. Dewald, and B. Moser.** 1997. Human chemokines: an update. Annu. Rev. Immunol. **15:**675–705.
4. **Barnes, P. J., and M. Karin.** 1997. Nuclear factor-κB: a pivotal transcription factor in chronic inflammatory diseases. N. Engl. J. Med. **336:**1066–1071.
5. **Bitko, V., A. Velazquez, L. Yank, Y.-C. Yang, and S. Barik.** 1997. Transcriptional induction of multiple cytokines by human respiratory syncytial virus requires activation of NF-κB and is inhibited by sodium salicylate and aspirin. Virology **232:**369–378.
6. **Brasier, A. R., M. Jamaluddin, A. Casola, W. Duan, Q. Shen, and R. Garofalo.** 1998. A promoter recruitment mechanism for TNF-α-induced IL-8 transcription in type II pulmonary epithelial cells: dependence on nuclear abundance of Rel A, NF-κB1 and c-Rel transcription factors. J. Biol. Chem. **273:**3551–3561.
7. **Brasier, A. R., M. Lu, T. Hai, Y. Lu, and I. Boldogh.** 2001. NF-κB-inducible BCL-3 expression is an autoregulatory loop controlling nuclear p50/NF-κB1 residence. J. Biol. Chem. **276:**32080–32093.
8. **Brasier, A. R., H. Spratt, Z. Wu, I. Boldogh, Y. Zhang, R. P. Garofalo, A. Casola, J. Pashmi, A. Haag, B. Luxon, and A. Kurosky.** 2004. Nuclear heat shock response and novel nuclear domain 10 reorganization in respiratory syncytial virus-infected A549 cells identified by high resolution 2D gel electrophoresis. J. Virol. **78:**11461–11476.
9. **Casola, A., R. Garofalo, M. Jamaluddin, S. Vlahopoulos, and A. R. Brasier.** 2000. Requirement of a novel upstream response element in respiratory syncytial virus-induced IL-8 gene expression. J. Immunol. **164:**5944–5951.
10. **Casola, A., R. P. Garofalo, H. Haeberle, T. Elliott, R. Lin, M. Jamaluddin, and A. R. Brasier.** 2000. Multiple inducible *cis* elements control RANTES promoter activation in alveolar epithelial cells infected with RSV. J. Virol. **75:**6428–6439.
11. **Casola, A., N. Burger, T. Liu, M. Jamaluddin, A. R. Brasier, and R. P. Garofalo.** 2001. Oxidant tone regulates RANTES gene expression in airway epithelial cells infected with respiratory syncytial virus. Role in viral-induced interferon regulatory factor activation. J. Biol. Chem. **276:**19715–19722.
12. **Choudhary, S., S. Boldogh, R. P. Garofalo, M. Jamaluddin, and A. R. Brasier.** 2005. RSV influences NF-κB-dependent gene expression through a novel pathway involving MAP3K14/NIK expression and nuclear complex formation with NF-κB2. J. Virol. **79:**8948–8959.
13. **Darnell, J. E., Jr., I. M. Kerr, and G. R. Stark.** 1994. Jak-STAT pathways and transcriptional activation in response to IFNs and other extracellular signaling proteins. Science **264:**1415–1421.
14. **Dechend, R., F. Hirano, K. Lehmann, V. Heissmeyer, S. Ansieau, F. G. Wulczyn, C. Scheidereit, and A. Leutz.** 1999. The Bcl-3 oncoprotein acts as a bridging factor between NF-κB/Rel and nuclear co-regulators. Oncogene **18:**3316–3323.
15. **Everard, M. L., A. Swarbrick, M. Wrightham, J. McIntyre, C. Dunkley, P. D. James, H. F. Sewell, and A. D. Milner.** 1994. Analysis of cells obtained by bronchial lavage of infants with respiratory syncytial virus infection. Arch. Dis. Child. **71:**428–432.
16. **Ferris, J. A., W. A. Aherne, and W. S. Locke.** 1973. Sudden and unexpected deaths to infants: histology and virology. Br. Med. J. **2:**439–449.
17. **Garofalo, R., M. Sabry, M. Jamaluddin, R. K. Yu, A. Casola, P. L. Ogra, and A. R. Brasier.** 1996. Transcriptional activation of the interleukin-8 gene by RSV infection in alveolar epithelial cells: nuclear translocation of the Rel A transcription factor as a mechanism producing airway mucosal inflammation. J. Virol. **70:**8773–8781.
18. **Haeberle, H., A. Casola, Z. Gatalica, S. Petronella, H.-J. Dieterich, P. B. Ernst, A. R. Brasier, and R. P. Garofalo.** 2004. IκB kinase is a critical regulator of chemokine expression and lung inflammation in respiratory syncytial virus infection. J. Virol. **78:**2232–2241.
19. **Hall, C. B., R. G. Douglas, Jr., K. C. Schnabel, and J. M. Geiman.** 1981. Infectivity of respiratory syncytial virus by various routes of inoculation. Infect. Immun. **33:**779–783.
20. **Han, Y., and A. R. Brasier.** 1997. Mechanism for biphasic Rel A:NF-κB1 nuclear translocation in tumor necrosis factor α-stimulated hepatocytes. J. Biol. Chem. **272:**9823–9830.
21. **Han, Y., T. Meng, N. R. Murray, A. P. Fields, and A. R. Brasier.** 1999. IL-1 induced NF-κB-IκBα autoregulatory feedback loop in hepatocytes: a role for PKCa in post-transcriptional regulation of IκBα resynthesis. J. Biol. Chem. **274:**939–947.
22. **Heissmeyer, V., D. Krappmann, F. G. Wulczyn, and C. Scheidereit.** 1999. NF-κB p105 is a target of IκB kinases and controls signal induction of BCL-3-p50 complexes. EMBO J. **18:**4766–4778.
23. **Jamaluddin, M., A. Casola, R. P. Garofalo, Y. Han, T. Elliott, P. L. Ogra, and A. R. Brasier.** 1998. The major component of IκBα proteolysis occurs independently of the proteasome pathway in respiratory syncytial virus-infected pulmonary epithelial cells. J. Virol. **72:**4849–4857.
24. **Kerr, L. D., C. S. Duckett, P. Wamsley, Q. Zhang, P. Chiao, G. Nabel, T. W. McKeithan, P. A. Baeuerle, and I. M. Verma.** 1992. The proto-oncogene bcl-3 encodes an I kappa B protein. Genes Dev. **6:**2352–2363.
25. **Kuwata, H., Y. Watanabe, H. Miyoshi, M. Yamamoto, T. Kaisho, K. Takeda, and S. Akira.** 2003. IL-10-inducible Bcl-3 negatively regulates LPS-induced TNF-α production in macrophages. Blood **102:**4123–4129.
26. **Li, X., S. Leung, S. Qureshi, J. E. Darnell, Jr., and G. R. Stark.** 1996. Formation of STAT1-STAT2 heterodimers and their role in the activation of IRF-1 gene transcription by interferon-alpha. J. Biol. Chem. **271:**5790–5794.
27. **Liu, T., S. Castro, A. R. Brasier, M. Jamaluddin, R. P. Garofalo, and A. Casola.** 2003. ROS mediate viral-induced stat activation: role of tyrosine phosphatases. J. Biol. Chem. **279:**2461–2469.
28. **May, M. J., and S. Ghosh.** 1997. Rel/NF-kappa B and I kappa B proteins: an overview. Semin. Cancer Biol. **8:**63–73.
29. **Na, S.-Y., J.-E. Choi, H.-J. Kim, B. H. Khun, J.-C. Lee, and J. W. Lee.** 1999. BCL-3, an IκB protein, stimulates activating protein-1 transactivation and cellular proliferation. J. Biol. Chem. **274:**28491–28496.
30. **Noah, T. L., F. W. Henderson, I. A. Wortman, R. B. Devlin, J. Handy, H. S. Koren, and S. Becker.** 1995. Nasal cytokine production in virus acute upper respiratory infection of childhood. J. Infect. Dis. **171:**584–592.
31. **Nowak, D. E., B. Tian, and A. R. Brasier.** Novel two-step cross-linking method for identification of NF-κB gene network by chromatin immunoprecipitation. BioTechniques, in press.
32. **Ohno, H., G. Takimoto, and T. W. McKeithan.** 1990. The candidate proto-oncogene bcl-3 is related to genes implicated in cell lineage determination and cell cycle control. Cell **60:**991–997.
33. **Oppenheim, J. J., C. O. C. Zachariae, N. Mukaida, and K. Matsushima.** 1991. Properties of the novel proinflammatory supergene "intercrine" cytokine family. Annu. Rev. Immunol. **9:**617–648.

34. **Pine, R.** 1997. Convergence of TNF-α and IFN-γ signalling pathways through synergistic induction of IRF-1/ISGF-2 is mediated by a composite GAS/κB promoter element. Nucleic Acids Res. **25:**4346–4354.
35. **Ray, S., S. Boldogh, and A. R. Brasier.** 2005. STAT3 NH_2-terminal acetylation is activated by the hepatic acute-phase response and required for IL-6 induction of angiotensinogen. Gastroenterology [Online.] doi:10.1053/j.gastro.2005.07.055.
36. **Richard, M., J. Louahed, J.-B. Demoulin, and J.-C. Renauld.** 1999. Interleukin-9 regulates NF-κB activity through BCL3 gene induction. Blood **93:** 4318–4327.
37. **Rocha, S., A. M. Martin, D. W. Meek, and N. D. Perkins.** 2003. p53 represses cyclin D1 transcription through down regulation of Bcl-3 and inducing increased association of the p52 NF-κB subunit with histone deacetylase 1. Mol. Cell. Biol. **23:**4713–4727.
38. **Ruuskanen, O., and P. L. Ogra.** 1993. Respiratory syncytial virus. Curr. Prob. Pediat. **2:**50–79.
39. **Schindler, C., and J. E. Darnell, Jr.** 1995. Transcriptional response to polypeptide ligands: the JAK-STAT pathway. Annu. Rev. Biochem. **64:**621–651.
40. **Shay, D. K., R. C. Holman, R. D. Newman, L. L. Liu, J. W. Stout, and L. J. Anderson.** 1999. Bronchiolitis-associated hospitalizations among US children, 1980–1996. JAMA **282:**1440–1446.
41. **Shay, D. K., R. C. Holman, G. E. Roosevelt, M. J. Clarke, and L. J. Anderson.** 2001. Bronchiolitis-associated mortality and estimates of respiratory syncytial virus-associated deaths among US children, 1979–1997. J. Infect. Dis. **183:**16–22.
42. **Sherman, C. T., and A. R. Brasier.** 2001. Role of STAT1 and STAT3 in inducible expression of the human angiotensinogen gene by interleukin-6. Mol. Endocrinol. **15:**441–457.
43. **Shiio, Y., J.-I. Sawada, H. Handa, T. Yamamoto, and J.-I. Inoue.** 1996. Activation of the retinoblastoma gene expression by Bcl-3: implication for muscle cell differentiation. Oncogene **12:**1837–1845.
44. **Sims, S. H., Y. Cha, M. F. Romine, P. Q. Gao, K. Gottlieb, and A. B. Deisseroth.** 1993. A novel interferon-inducible domain: structural and functional analysis of the human interferon regulatory factor 1 gene promoter. Mol. Cell. Biol. **13:**690–702.
45. **Springer, T.** 1994. Traffic signals for lymphocyte recirculation and leukocyte emigration: the multiple paradigm. Cell **76:**301.
46. **Sun, S. C., P. A. Ganchi, D. W. Ballard, and W. C. Greene.** 1993. NF-kappa B controls expression of inhibitor I kappa B alpha: evidence for an inducible autoregulatory pathway. Science **259:**1912–1915.
47. **Sun, S. C., P. A. Ganchi, C. Beraud, D. W. Ballard, and W. C. Greene.** 1994. Autoregulation of the NF-kappa B transactivator RelA (p65) by multiple cytoplasmic inhibitors containing ankyrin motifs. Proc. Natl. Acad. Sci. USA **91:**1346–1350.
48. **Tam, W. F., L. H. Lee, L. Davis, and R. Sen.** 2000. Cytoplasmic sequestration of rel proteins by IκBα requires CRM1-dependent nuclear export. Mol. Cell. Biol. **20:**2269–2284.
49. **Thanos, D., and T. Maniatis.** 1995. Virus induction of human IFN beta gene expression requires the assembly of an enhanceosome. Cell **83:**1091–1100.
50. **Thomas, L. H., J. S. Friedland, M. Sharland, and S. Becker.** 1998. Respiratory syncytial virus-induced RANTES production from human bronchial epithelial cells is dependent on nuclear factor-κB binding and is inhibited by adenovirus-mediated expression of inhibitor of κBα. J. Immunol. **161:**1007–1016.
51. **Tian, B., Y. Zhang, B. A. Luxon, R. P. Garofalo, A. Casola, M. Sinha, and A. R. Brasier.** 2002. Identification of NF-κB-dependent gene networks in respiratory syncytial virus-infected cells. J. Virol. **76:**6800–6814.
52. **Tian, B., D. E. Nowak, M. Jamaluddin, S. Wang, and A. R. Brasier.** 2005. Identification of direct genomic targets downstream of the NF-kappa B transcription factor mediating TNF signaling. J. Biol. Chem. **280:**17435–17448.
53. **Uduman, S. A., M. K. Ijaz, J. Kochiyil, T. Mathew, and M. K. Hossam.** 1996. Respiratory syncytial virus infection among hospitalized young children with acute lower respiratory illnesses in Al Ain, UAE. J. Communicable Dis. **28:**245–252.
54. **Virca, G. D., W. Northemann, B. R. Shiels, G. Widera, and S. Broome.** 1990. Simplified Northern blot hybrdization using 5% sodium dodecyl sulfate. BioTechniques **8:**370–371.
55. **Vlahopoulos, S., I. Boldogh, and A. R. Brasier.** 1999. NF-κB-dependent induction of interleukin-8 gene expression by tumor necrosis factor α: evidence for an antioxidant sensitive activating pathway distinct from nuclear translocation. Blood **94:**1878–1889.
56. **Wessells, J., M. Baer, H. A. Young, E. Claudio, K. Brown, U. Siebenlist, and P. F. Johnson.** 2004. BCL-3 and NF-κB p50 attenuate lipopolysaccharide-induced inflammatory responses in macrophages. J. Biol. Chem. **279:**49995–50003.
57. **Wormald, S., and D. J. Hilton.** 2004. Inhibitors of cytokine signal transduction. J. Biol. Chem. **279:**821–824.
58. **Wulczyn, F. G., M. Naumann, and C. Scheidereit.** 1992. Candidate proto-oncogene bcl-3 encodes a subunit-specific inhibitor of transcription factor NF-kappa B. Nature **358:**597–599.
59. **Zhang, L., M. E. Peeples, R. C. Boucher, P. L. Collins, and R. J. Pickles.** 2002. Respiratory syncytial virus infection of human airway epithelial cells is polarized, specific to ciliated cells, and without obvious cytopathology. J. Virol. **76:**5654–5666.
60. **Zhang, M.-Y., E. W. Harhaj, L. Bell, S.-C. Sun, and B. A. Miller.** 1998. BCL-3 expression and nuclear translocation are induced by granulcotye-macrophage colony-stimulating factor and erythropoietin in proliferating human erythroid precursors. Blood **92:**1225–1234.
61. **Zhang, Q., J. A. DiDonato, M. Karin, and T. W. McKeithan.** 1994. BCL3 encodes a nuclear protein which can alter the subcellular location of NF-κB proteins. Mol. Cell. Biol. **14:**3915–3926.
62. **Zhang, Y., B. A. Luxon, A. Casola, R. P. Garofalo, M. Jamaluddin, and A. R. Brasier.** 2001. Expression of RSV-induced chemokine gene networks in lower airway epithelial cells revealed by cDNA microarrays. J. Virol. **75:** 9044–9058.
63. **Zhong, H., M. J. May, E. Jimi, and S. Ghosh.** 2002. The phosphorylation status of nuclear NF-κB determines its association with CBP/p300 or HDAC-1. Mol. Cell **9:**625–636.